University of Groningen

Improved value and carbon footprint by complete utilization of corncob lignocellulose

Pang, Bo; Sun, Zhuohua; Wang, Lei; Chen, Wei Jing; Sun, Qian; Cao, Xue Fei; Shen, Xiao Jun; Xiao, Lin; Yan, Jin Long; Deuss, Peter J.

IMPORTANT NOTE: You are advised to consult the publisher's version (publisher's PDF) if you wish to cite from it. Please check the document version below.

Document Version
Publisher's PDF, also known as Version of record

Publication date:
2021

[Link to publication in University of Groningen/UMCG research database](#)

Improved value and carbon footprint by complete utilization of corncob lignocellulose

Bo Pang [a,1], Zhuohua Sun [a,1], Lei Wang [b,c,1], Wei-Jing Chen [a], Qian Sun [a], Xue-Fei Cao [a], Xiao-Jun Shen [d], Lin Xiao [e], Jin-Long Yan [e], Peter J. Deuss [f], Tong-Qi Yuan [a,*], Run-Cang Sun [g,*]

[a] Beijing Advanced Innovation Center for Tree Breeding by Molecular Design, Beijing Key Laboratory of Lignocellulosic Chemistry, Beijing Forestry University, Beijing 100083, China
[b] Key Laboratory of Coastal Environment and Resources of Zhejiang Province (KLaCER), School of Engineering, Westlake University, Hangzhou 310024, Zhejiang Province, China
[c] Institute of Advanced Technology, Westlake Institute for Advanced Study, Hangzhou 310024, Zhejiang Province, China
[d] Beijing National Laboratory for Molecular Sciences, CAS Key Laboratory of Colloid and Interface and Thermodynamics, CAS Research/Education Center for Excellence in Molecular Sciences, Institute of Chemistry, Chinese Academy of Sciences, Beijing 100190, China
[e] Shandong Key Laboratory of Straw and Stover Biorefinement Technologies, Shandong Longlive Bio-technology Co., Ltd., Dezhou 251200, Shandong Province, China
[f] Department of Chemical Engineering (ENTEG), University of Groningen, Groningen 9747 AG, the Netherlands
[g] Center for Lignocellulose Chemistry and Materials, Dalian Polytechnic University, Dalian 116034, Liaoning Province, China

ARTICLE INFO

ABSTRACT

Lignocellulose, as the most abundant type of inedible biomass, is considered as a promising renewable feedstock for making fuels, chemicals, and materials. However, its complex structure makes most of current biorefinery processes suffer from low resource utilization rates, high energy consumption or ill-defined market orientation of the obtained products. Here, we propose and evaluate the EXA (Ethanol, Xylose, Adhesive) biorefinery strategy based on current xylose industry. This process integrates four conversion and separation stages to consecutively produce ethanol, xylose, and adhesive with total carbon utilization of 79.6%. The key innovation is the establishment of an easy-to-operate process for direct production of high-quality adhesive from a lignin-rich liquid fraction that makes the overall process significantly more sustainable. Techno-economic analysis (TEA) shows that the revenue of proposed EXA process increases more than 110 times compares with the current process and life cycle assessment (LCA) demonstrates a much lower CO_2 footprint from an environmental burden per unit of revenue perspective.

1. Introduction

With the increasing demand for chemicals, fuels, and materials in our global society, the efficient and sustainable exploitation of renewable resources is recognized as the key for future sustainable development [1–3]. In this context, the utilization of lignocellulose, the most abundant and wide-spread renewable resource on our earth, has attracted great attention in recent years [4]. Furthermore, lignocellulose has been projected as the most important carbon–neutral resource for decreasing CO_2 emissions and atmospheric pollution [5,6]. However, due to its complex structure, efficient and complete utilization of all lignocellulose components for producing valuable products is a challenge. Therefore, the development of cost-effective and environmental-friendly

approaches that lead to the production of a product portfolio that aligns with the current chemicals and materials market needs to be addressed [7,8].

Typically, current industrial processes targeting valorization of lignocellulose mainly focus on the application of the carbohydrate part, as for example in the paper and cellulosic ethanol industry [9,10]. In these processes, the produced condensed lignin streams are considered as by-products and normally burned to generate heat [11] or converted to bio-based fuels via energy-intensive catalytic processes [12,13]. In order to make the most use of all lignocellulose components, especially to improve the value of lignin stream, various strategies targeting total valorization of lignocellulose have been developed in recent years [14]. The first upcoming strategy that has aroused great interest in recent
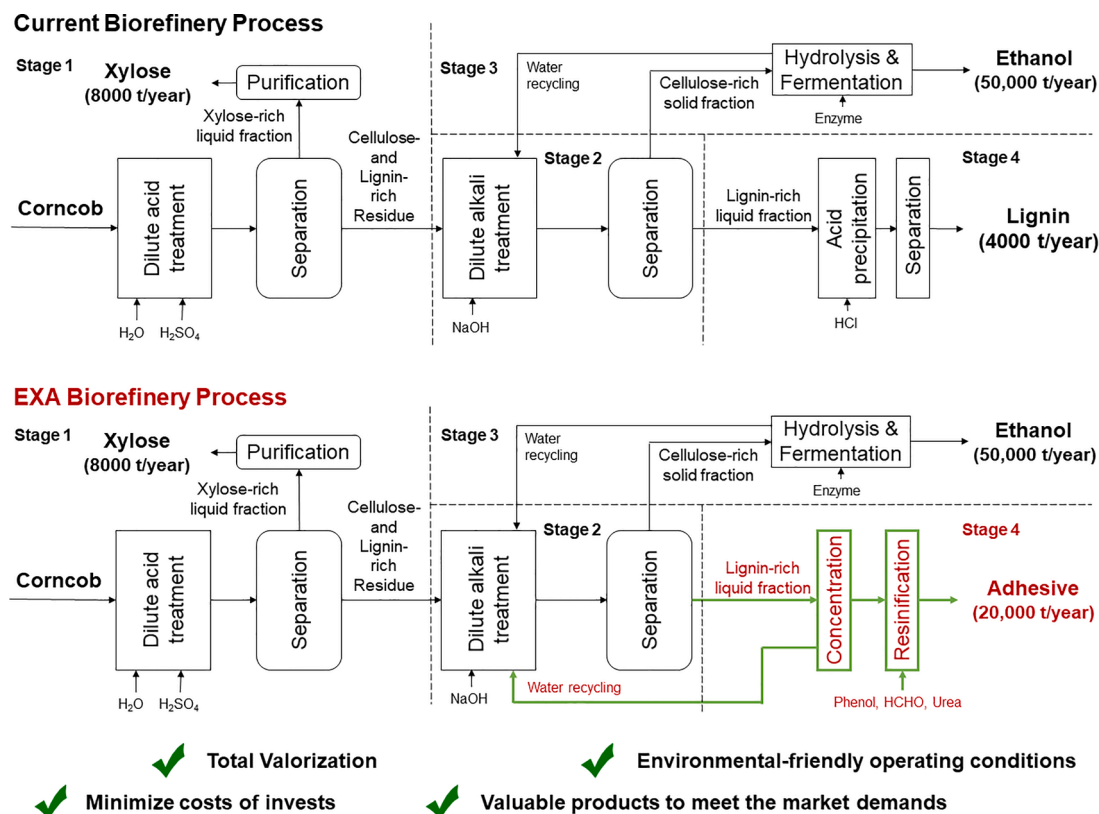

Fig. 1. General scheme of current xylose biorefinery process as operated by Shandong Longlive Biotechnology Co., Ltd. (top) and the proposed EXA biorefinery process for total valorization of corncob lignocellulose (bottom).

years relies on the development of efficient lignin isolation with minimal structural degradation to allow for the generation of high yields of selected high-value lignin monomers [15–17]. An example is the process of adding formaldehyde during organosolv pretreatment to provide a soluble lignin fraction and which allows for the further depolymerization of cellulose, hemicelluloses and lignin separately to achieve the complete valorization of all components [18]. A second strategy relies on converting the whole lignocellulosic material in one- pot, which significantly reduces the complexity of the whole process [14]. However, the diversity of products obtained from each component in lignocellulose brings great difficulties in the system design. So far, only a few examples have been reported and most of these operated via energy intensive catalytic systems and produce complex mixtures of products that cannot be applied as such and thus require complex separation steps [19–21]. A third approach has been developed in recent years and integrates lignin isolation with effective in-situ catalytic depolymerization [22–28]. Compared with the two other processes, this process can deliver lignin monomers in high yields and excellent polysaccharide retention and digestibility potential [27]. However, significant cost reductions of the energy intensive depolymerization process and establishment of a market for produced lignin monomers need to be addressed in the future [28,29]. Additionally, these processes do not have a good strategy for dealing with the hemicellulose component as it typically degrades together with lignin and thus complicates downstream processing and lowers the carbon utilization efficiency.

Thus, the development of a sustainable process that is able to compete economically with petroleum refineries is still difficult due to the vast investment cost and ill-defined market orientation of the produced products. Compared with other processes focusing on either lignin or cellulose first, production of valuable compounds from hemicellulose derived from lignocellulose is also possible. The generated products are normally C5 sugars [30,31] or furfural [32]. Recently, a biorefinery process based on this strategy was developed, in which

hemicellulose from corncob was firstly converted into xylose by well-known dilute acid treatment (Fig. 1) and then the solid residue was isolated and further used for the production of bioethanol while leaving the recovered solid lignin for use in other applications. Currently, this process operates with an annual production of 8000 t xylose, 50000 t ethanol and 4000 t lignin per year. However, during this process the lignin valorization has not yet been adequately developed. Although, lignin could be sold for other process, such as the production of biochar [33], the impurities remaining in lignin make further processing more complicated. Moreover, the lignin separation process used large amounts of acid and the generated large amount of waste water which leads to additional environmental problems. Without overcoming this challenge, the revenue of current process is only 12.71 USD for each 1.00 t fuel ethanol produced from lignocellulose.

In this context, herein we successfully developed the EXA (Ethanol, Xylose, Adhesive) biorefinery process based on the hemicellulose-first biorefinery process which addresses the trickiest issue of lignin utilization by direct valorization as a lignin-based phenol formaldehyde (LPF) resin adhesive without any further treatment. Moreover, a waste water recycling system was introduced that allowed to reduce pollution issues. Overall, the EXA biorefinery process was developed based on the principles listed in Fig. 1 which can be described as: 1. The complete and efficient valorization of all lignocellulose components; 2. The direct entry into a current industrial process to minimize costs of invests; 3. The operation under environmental-friendly conditions; 4. The production of valuable products with direct market entries.

The proposed EXA biorefinery strategy which produces ethanol, xylose, and adhesive as end products and results in the total valorization of all lignocellulose components. Importantly, every lignocellulose components after fractionation were directly valorized during EXA biorefinery. According to LCA and TEA, this easy-to-operate process was cost- and eco-efficient and environmental-friendly, while achieving the efficient exploitation of all lignocellulosic biomass components.

Meanwhile, the value-added products (xylose, ethanol, and adhesive) from lignocellulose can be directly commercialized with economic competitiveness and negligible market risk.

2. Materials and methods

2.1. Materials

Corncob and cellulose- and lignin-rich residue were obtained from Shandong Longlive Biotechnology Co., Ltd (Shandong Province, China). All other chemicals used in this study were purchased from Beijing Chemical Works.

2.2. Analytical methods

2.2.1. Compositional and elemental analysis

Compositional analysis was carried out according to the standard laboratory analytical procedures NREL/TP-510-42618 [34]. The compositions of corncob, cellulose- and lignin-rich residue, the cellulose fraction after dilute alkali treatment, and the residue after fermentation are listed in Table S1. Elemental analysis was acquired on an elementar vario Micro cube (Elementar, Germany).

2.2.2. Characterization of lignin

The molecular weights of L_2 samples were determined by gel permeation chromatography 1200 (Agilent, U.S.). The lignin sample was directly dissolved in THF without any other treatment. The nuclear magnetic resonance (NMR) analyses were acquired on a Bruker AVIII 400 MHz spectrometer (Bruker, Germany) at 25 °C. The instrument parameters were set based on the previous study [35,36].

2.2.3. Characterization of lignin-based phenol formaldehyde (LPF) resin adhesives

A Bruker AV-III 400 MHz spectrometer (Bruker, Germany) was used to record the ^{13}C NMR spectra of the LPF resin adhesives at 25 °C. 80 mg freeze-dried uncured resins were dissolved in 0.5 mL of D_2O. The differential scanning calorimeter (DSC) analysis of the uncured freeze-dried resins was acquired on DSC214 (Netzsch, Germany). The heating rates of scans were set at 5 °C min^{-1}, 10 °C min^{-1}, and 15 °C min^{-1} respectively. Thermal stability of the LPF resin adhesives were measured with a TGA/DSC 1600 (Mettler Toledo, Switzerland). Curves of the weight loss and the derivative weight loss (DTG) were plotted. The physical properties of the LPF resin adhesives were determined in accordance with the Chinese National Standard (GB/T 14074–2017).

The performances of the LPF resin adhesives were tested via its application as an adhesive in plywood according to the Chinese National Standard (GB/T 17657–1999). The three-layers laboratory plywood panels (400 mm × 400 mm × 6.6 mm) were produced using LPF resin adhesives (L_1PF mixed with 14.54% fermentation residue and 5.46% wheat flour and as filler, L_2PF mixed with 20.00% wheat flour and as filler) and poplar veneers. The glue spread was 316 g m^{-2} of the double glue line. The plywood was hot-pressed at 145 °C under 1.0 MPa for 594 s (90 s mm^{-1}). The bonding strength was tested using a universal testing machine after the samples (100 mm × 25 mm) being boiled in water at 100 °C for 3 h. The formaldehyde emission was tested according to the desiccator method with the samples 150 mm × 50 mm.

2.3. Approach to producing adhesives

The L_1PF resin adhesive was synthesized using the concentrated liquid lignin fraction (L_1) with lignin content of 33.20%. The 50% substitution rate of lignin to phenol (calculated based on the lignin content) and a mol ratio of phenol to formaldehyde of 1.0:1.8 was used. In the first step, phenol was mixed with the liquid lignin fraction in a three-necked flask. The residual NaOH left in the lignin fraction from previous dilute alkali treatment step resulted in an alkali environment.

The quantity of NaOH in this lignin rich solution was approximately 30%, which meant much less NaOH was needed when using the lignin solution compared with an isolated lignin as feedstock. The mixture was heated at 90 °C for 1 h. Next, the NaOH solution (30 wt%) and 70% of the total formaldehyde was added with the mixture heating at 80 °C for 1 h. Finally, the NaOH solution (30% wt) and urea (5 wt% of phenol) was then added after the temperature dropped to 65 °C.

The L_2PF resin adhesive was synthesized using the solid lignin (L_2) obtained via acidic precipitation and separation from concentrated lignin fraction. Before the preparation, L_2 was dried overnight in an oven at 60 °C. The L_2PF resin adhesive was produced with a solid lignin substitution rate of 50% (in relation to the mass of phenol). Similar to the L_1PF resin adhesive preparation procedure, in the first step, phenol and L_2 were mixed in a three-necked flask. Then, the appropriate amount of NaOH solution (30% wt) was added to adjust the pH value to 9–10. The subsequent process was in accordance with that of the preparation of the L_1PF resin.

2.4. Techno-economic analyses

The techno-economic analyses were performed based on a plant-size process model of producing 1 t ethanol. Most of the data were provided by Shandong Longlive Biotechnology Co., Ltd. (Shandong, China) which is one of the first companies that had obtained the qualification of China to produce bioethanol from 2005 and some steps related to L_1PF resin were slightly adjusted according to the existing industry. These practical data were the mean value from two years operations (2016–2017).

2.5. Life cycle assessment

Life cycle assessment approach (LCA) is an environmental tool assessing the impact on the environment of a product or a process through its life cycle [37]. LCA was performed to quantify the greenhouse gas (GHG) intensities during these two processes. The "cradle-to-gate" system boundaries of the current and the proposed integrated biorefinery include collection, transportation of corncob, and biorefinery process. Because corncob is the waste from corn harvest, the environmental burdens related to growth and harvest are allocated to corn completely. According to the literature, it is assumed that every 1.0 kg of corn produced provides 0.15 kg of corncobs and the diesel consumption is 1300 MJ/acre on average [38]. The transportation of corncob is done by diesel driven truck for approx. 50 km, from the storage to biorefinery plant within the Shandong province. Land use change and infrastructures are not included in their system boundaries. Carbon intensity or greenhouse gas (GHG) intensity, as either GHG emissions per unit of product or per plant was selected as the environmental indicator to compare current and EXA processes. Since the EXA process was upgrade with water recycling system, water usages were also highlighted for two systems.

Functional units for both designs are "to process 5.25 t corncob", equivalent to 1.00 t ethanol, 0.75 t xylose, and 2.14 t lignin or 6.00 t LPF resin adhesive. Results are shown as kg CO_2 eq./ kg or MJ of products from biorefineries. The biorefinery is a multi-products system and therefore the allocation was applied among these products following the economic allocation approach, with surplus electricity from anaerobic digestion as an exception. Surplus electricity is treated by system expansion method, as a substitution of the grid mix. The allocation proportions were estimated and explained in the Results section. A "2%" cut-off criteria is applied, which means that any input below 2% of the main output ethanol was excluded from the calculation. In addition to results interpretation, contribution analysis ("hot spot" analysis), sensitivity analysis and scenario analysis for further carbon intensity improvement opportunities were also performed.

Inventory data for chemicals, electricity and coal based steam is from the China LCA core database (CLCD) embedded in WebLCA software [39]. Inventory data for natural gas based steam in EU-28 and biomass

based steam in China is from Gabi database, and those for yeast and cellulase enzyme is from the GREET 2018 model [40]. Inventory data for wastewater effluents offsite treatment is from the Ecoinvent v3.1 database embedded in WebLCA software. GHG intensities for all products were calculated based on the IPCC AR4 [41] method using conversion factor 298 for N_2O and 25 for methane. The calculation was done using an in-house developed excel based spreadsheet.

3. Results and discussion

3.1. The EXA biorefinery processing stages

As shown in Fig. 1, both current biorefinery process and the EXA biorefinery process contain four stages. Stage 1 focuses on depolymerization of hemicellulose to xylose and solid liquid separation. The residue after xylose production is mainly composed of cellulose (60.5%) and lignin (29.0%). Stage 2 is the processing of cellulose- and lignin-rich residue, for which dilute alkali treatment is used to separate these two fractions for further utilization. Stage 3 refers to valorization of cellulose to ethanol. The cellulose fraction after dilute alkali treatment contains 87.3% cellulose that can be used for the direct enzymatic hydrolysis and fermentation to obtain ethanol. Stage 4 is the valorization of the lignin-rich fraction to adhesive in the EXA process or isolation of lignin for the current process. Innovations presented in this manuscript lie with the modification of stage 4 in which the lignin-rich fraction is directly used for phenol–formaldehyde adhesives without the need for further purification as well as alkali liquid waste treatment.

The designed production capacity of current process is 8000 t/year for xylose, 50, 000 t/year for ethanol, and 4000 t/year for lignin. The production capacity of adhesive (20, 000 t/year) was estimated based on that of lignin. For a more detailed comparison of the processing procedures with mass balances, see Figs. S1 and S2.

3.1.1. Depolymerization of hemicellulose to xylose

Depolymerization of hemicellulose to xylose (Fig. 1, Stage 1) is already a mature process that has been industrialized for several decades. Over the years, the application of xylose has grown dramatically in food, beverages, and pharmaceuticals [42]. Its market reached about 1.5 billion dollars in 2018 [43]. Various feedstocks including corncob [44,45], corn stover [46], sugarcane [47], and wheat straw [31] have shown potential for direct production of high yield xylose without prior separation of hemicellulose. Corncob with high hemicellulose content (31.8%, Table S1) is an abundant and cheap resource with annual production of 250 million tons as agricultural waste [48]. Cost-effective and

sustainable production of valuable products from corncob has attracted great attention in recent years [48–50] and it was therefore selected as feedstock to demonstrate the EXA biorefinery.

The depolymerization of hemicellulose was done in a dilute H_2SO_4 solution. Following separation and purification, marketable high-quality xylose is obtained (Fig. S1). Processing and valorization of the cellulose- and lignin-rich residue (Fig. 1, Stage 2) starts with the separation of the two main components in stage 2. The selected integrated treatment and separation process allows to take the maximum advantage of the chemical structures of each biopolymer and is optimal for the target products. Dilute alkali treatment was applied owing to its efficient delignification, convenient operation, and the fact that it is commercially well established. The wet cellulose- and lignin-rich residue could be directly treated with a high feedstock loading. A cellulose-rich fraction was isolated as solid and could be separated from the lignin-rich liquor. The lignin fraction contains only a trace amount of residual carbohydrates (0.41%) and has a M_w of 1220 g mol^{-1}. Two variations of lignin; L_1 (concentrated lignin-rich liquor) and L_2 (purified solid lignin obtained by precipitation used as a control) were investigated by GPC, FT-IR spectroscopy, 2D HSQC NMR spectra, ^{31}P NMR and ^{13}C NMR. (See Figs. S3–S6, Tables S2–S5 for detailed discussion).

3.1.2. Production of bioethanol

For the efficient production of bioethanol, it is important that the obtained cellulose is of sufficient purity. Herein, we are aiming to produce high purity ethanol via an integrated enzymatic hydrolysis and fermentation process (Fig. 1, Stage 3) [51]. Globally, bioethanol is an important sustainable source of energy and is also in high demand in China. But so far, the production capabilities in China (2.68 million tons in 2018) are still far below the 2020 production target (10 million tons) set by the nation's Long and Mid-Term Planning for Renewable Energy Plan. In this work, the enzymatic hydrolysis and fermentation process were conducted continuously in a single reaction still. The fermentation was performed at 38 °C for 72 h. The mixture obtained after fermentation was then separated yielding high purity ethanol (1.0 t). It is noteworthy that there were some solid hydrolysis residues left after the enzymatic hydrolysis process. Previously, these residues were usually treated as the solid waste that was burned to provide energy. To achieve maximum benefits, these hydrolysis residues are proposed to be used as the filler of LPF resin adhesives in this improved strategy (see main text below).
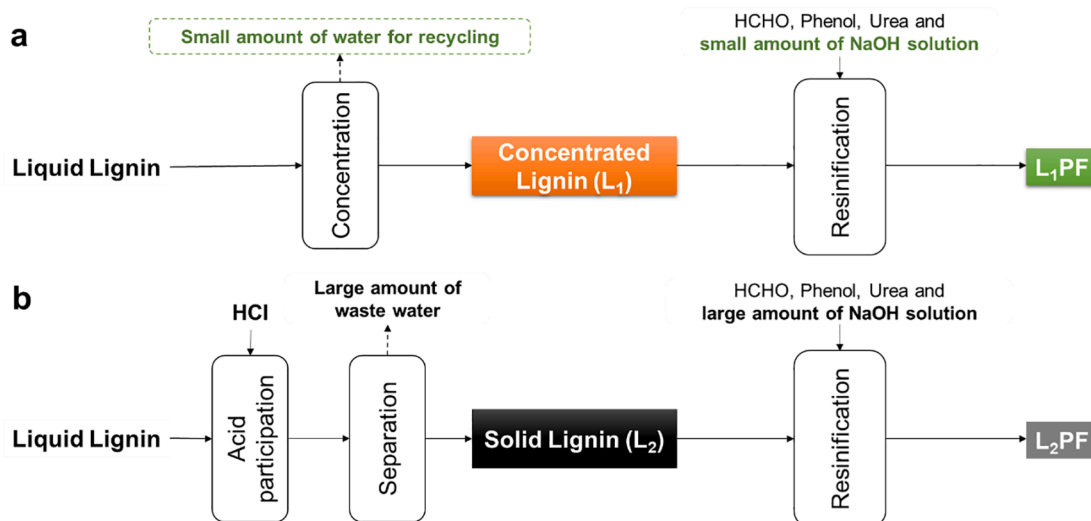

Fig. 2. Schematic representation of the production processes for the L_1PF (a) and L_2PF (b) resin adhesives.
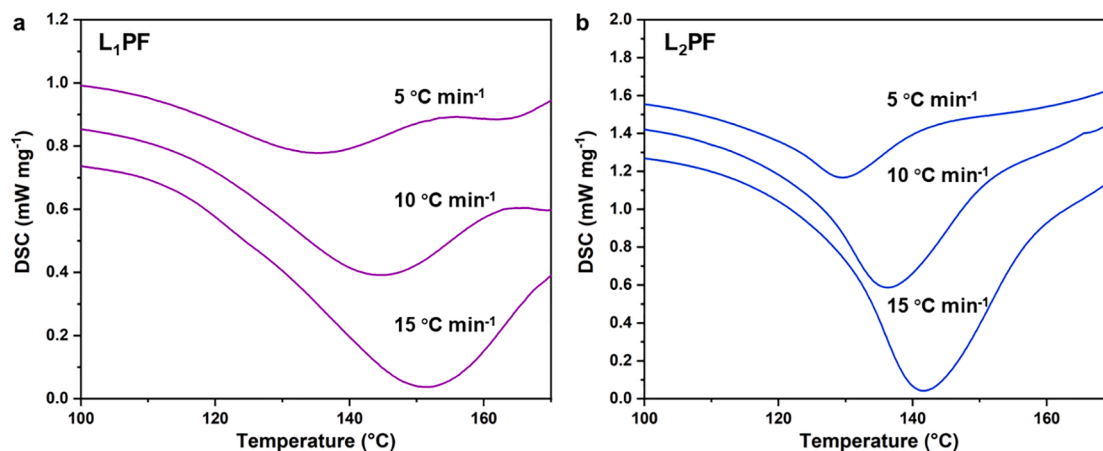
Fig. 3. Differential Scanning Calorimetry (DSC) analyses of produced LPF resin adhesives.

3.1.3. From lignin to lignin-based phenol formaldehyde (LPF) resin adhesives

The next important step was the utilization of lignin (Fig. 1, Stage 4), the main component in the lignin-rich liquor. Although the lignin obtained in this process has been valorized into a range of niche products [15–17]. However, most of these are hard to be commercialized owing to the high costs or uncertain market requirements. Lignin is also considered as a renewable source of phenolics to (partly) replace phenol for the production of phenolic resins [52–54]. The formed resins from lignin normally perform weak reactivity due to their higher steric hindrance. Herein, we put forward our focus on the market of wood adhesives as it has the largest market share and is driving phenolic resin consumption on a global scale [55]. The global wood adhesive market size has reached USD 4.60 billion in 2018 and is predicted to keep growing from 2019 to 2025 with approximately 4.7% annually [56].

The lignin fraction after alkaline treatment was concentrated to 60% solid content, while for lignin the weight content is 33.2%. The carbohydrate contents of the alkali-soluble lignin (L_2) are only 0.41%. This low content of carbohydrate (<1%) shows the high purity of this lignin which is good enough to sell as the final product for further application. The M_w of L_2 was 1220 g mol^{-1} showing very limited condensation. The polydispersity of 1.07 indicated that the alkali-soluble lignin was homogeneously dispersed in the THF solution.

Traditionally, the lignin used to prepare resins is usually purified first to decrease the adverse effects from carbohydrates and other impurities on the adhesive properties. Previously, we have reported the valorization of technical lignin [57,58] as well as bioethanol fermentation residues [59] for the production of desirable resins with high substitution rate and controllable viscosity. Further application of LPF resin adhesives in large scale via our developed technology for the production of plywood in China demonstrated an innovative costs reduction strategy for related industrial processes [60]. However, the conventional approach needs to use a large quantity of acid for precipitating lignin, which makes the further separation method rather complex and produces plenty of waste water that is difficult for further recycling and post-processing steps. Because of the prior hemicellulose removal, the proposed EXA strategy allows for the direct use of the liquid lignin-rich fraction without the need of an extra separation step. Therefore, it also avoids the additional generation of waste required for the purification. Solely, an ordinary concentration step that keeps around 60.0% solid content was applied to facilitate the preparation of lignin-based phenolic resins and avoided the use of a complex separation process (Fig. 2a). To further improve the overall efficiency of the whole process, the recovered distilled water was recycled to wash the solid fraction after dilute alkali treatment (Fig. S2).

3.1.4. Chemical structure analysis of the uncured LPF resin adhesives

For comprehensive and better understanding of the properties of produced adhesives, two types of LPF resin adhesives were prepared as shown in Fig. 2. L_1PF resin adhesive was prepared directly from the lignin-rich liquor after concentration and L_2PF resin adhesive was prepared from the solid lignin isolated by acid precipitation. The properties of LPF resin adhesives are determined by its chemical structures, which is also investigated with solution-state ^{13}C NMR. Fig. S7 displays the spectra and the signals were analyzed based on the existing literatures [61–64].

The carbonyl groups of the substituted urea are 162.2 ppm (monosubstituted) and 160.1 ppm (disubstituted). The higher intensity of peaks which belong to substituted urea in L_1PF resin adhesive indicated that there is slightly more unreacted formaldehyde in this system. The signals from 133.0 to 125.0 ppm represent the reacted aromatic carbons in lignin and phenol. The peaks of the substituted *para* (129.8 ppm) and *ortho* (127.2 ppm) C–C sites of LPF resin adhesives were very similar. The series of peaks from 118.7 to 114.8 ppm belong to the unsubstituted aromatic carbons. The peak at 118.2 ppm represents the unsubstituted *para* carbons, which implied that the amount of unreacted phenol in L_1PF resin adhesive was higher than another one.

The peaks at 71.6 ppm (*para*) and 68.9 ppm (*ortho*) are the benzylether groups between aromatic rings, which only existed in L_1PF resin adhesive. The methylene ether bridge is not detected as it is unstable during the curing process. The signals of methylol group condensed between urea and formaldehyde were at 65.3 ppm (*para*) and 62.0 ppm (*ortho*), respectively. These kinds of bridges mainly existed in L_1PF resin, especially the *ortho*-NH-CH$_2$OH bonds. The peaks at 63.7 ppm (*para*) and 61.0 ppm (*ortho*) are the methylol groups on the aromatic rings, which means the L_2PF resin adhesive suffered more condensation reactions between aromatic rings and formaldehyde. Traditionally, the *para* site of phenolic rings is more reactive than the *ortho* sites. The strong signals at 61.0 ppm indicated that there were considerable reactive sites of lignin participating in the condensation reaction. The peaks at 60.5 ppm and 55.5 ppm represent the methylene groups between urea. Therein, the -N(CH$_2$–)CH$_2$-N(CH$_2$)- bridge in L_1PF resin adhesive was obviously more than that in L_2PF resin adhesive. The signals at 39.0 ppm and 34.0 ppm are the methylene groups between aromatic rings. In general, the condensation degree of L_2PF resin adhesive was more thorough. There are still some condensation reactions that occurred at the initial stage, which correlated with the steric hindrance generated by the impurities in the concentrated liquid. In addition, there are also some unstable linkages in L_1PF resin adhesive, which can affect the properties of the final plywood.

3.1.5. Curing kinetics of the LPF resin adhesives

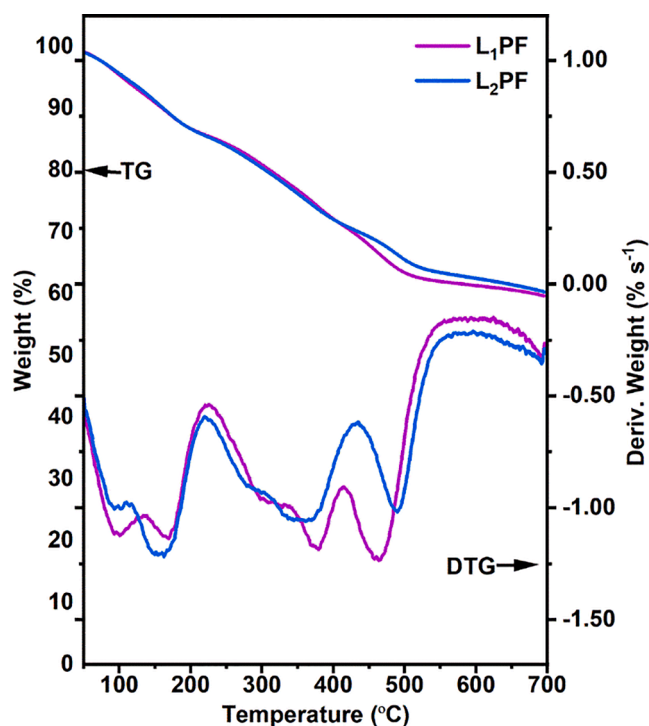The curing process of the produced adhesives has a major influence

Fig. 4. Differential thermogravimetric (DTG) and thermogravimetric (TG) analysis of produced LPF resin adhesives.

Table 1
Properties of produced LPF resin adhesives.

Samples	Solid content (%)	pH (25 °C)	Viscosity (22 °C, mPa·s)
L₁PF	52.38%	11.6	632.6
L₂PF	51.47%	11.5	1630.0
GB/T[a]	≥35.0	≥7.0	≥60.0

[a] Test method based on the Chinese standard GB/T 14732-2017.

on plywood performance. DSC was used to analyze the curing kinetics of the LPF resin adhesives [54]. The activation energy data were calculated by both the Kissinger (1) and Flynn-Wall-Ozawa (2) methods:

$$\ln\left(\frac{\beta}{T_P^2}\right) = \ln\frac{A_0 R}{E_k} - \frac{E_k}{RT_P} \tag{1}$$

$$\log\beta = -2.315 - 0.4567\left(\frac{E_f}{RT_P}\right) + \log\left(\frac{A_0 E}{R}\right) - \log\left(\int_{\alpha_0}^{\alpha_P} \frac{1}{f(\alpha)}d\alpha\right) \tag{2}$$

The results obtained are given in Fig. 3 and Table S6.

The characteristic curing temperature of L₁PF resin adhesive (128.5 °C) was slightly higher than that of L₂PF resin adhesive (122.7 °C). The chemical structures of both adhesives correlate crucially with the curing temperature. As shown in Fig. 3, the intensities of the unsubstituted carbons of L₂PF resin adhesive are markedly lower than another one, which resulted in a lower curing temperature of L₂PF resin adhesive [58].

3.1.6. Thermal decomposition of LPF resin adhesives

The thermal stability of resin is highly dependent on the synthesis conditions and the molecular structure of resins [65]. TG detection was used in this study to analyze the produced adhesives. The results are presented in Fig. 4 and Table S7. The initial stage of ∼ 11% weight loss was primarily owing to the evaporation of the water and remaining formaldehyde. The principal mass loss event occurred during the second stage between 221 and 320 °C. This decomposition took place via the partial breakdown of the methylene and methylol linkages [66,67]. The

Table 2
Performances of the plywood using LPF resin adhesives.

Samples	Bonding strength (MPa)	Formaldehyde emission (mg L⁻¹)
L₁PF	0.87	0.08
L₂PF	1.09	0.07
China[a]	≥0.70	≤1.50
ISO	0.00–1.00[b]	≤0.50[c]
Japan	≥0.70[d]	≤0.30[e]

[a] Test method based on the GB/T 17657. The formaldehyde emission class is E₁.
[b] Test method based on the ISO 12466. The mean shear strength is between 0.00 and 1.00 MPa when the average apparent cohesive wood failure is 100–40%.
[c] Test method based on the ISO 12460. The formaldehyde emission class is E₁.
[d] Test method based on the JAS MAFF.
[e] Test method based on the JIS A 1460. The formaldehyde emission class is F☆☆☆☆ (JAS 233: 2008).

third and fourth stages occurred between 320 and 434 °C and 434–549 °C, respectively. The fragmentation of the side chains present in lignin and the methylene bridges leading to the weight loss [66,68]. These results indicate that the thermal stability of different adhesives was approximate owing to their similar chemical composition.

3.1.7. Performances of the plywood produced by LPF resin adhesives

As shown in Table 1, the solid content of L₁PF resin adhesive was slightly higher than that of L₂PF resin adhesive. 8.41% NaOH was left in the lignin fraction L₁ after alkaline treatment and the following concentration step. Therefore, the amount of NaOH used in the first processing step of L₁PF resin adhesive production was reduced correspondingly to keep a similar pH value of the final LPF resin adhesives. The viscosity of L₁PF resin adhesive was markedly lower than that of L₂PF resin adhesive. The feedstock L₁ was the liquid fraction with 40% water that decreased the viscosity of the circumstances. In addition, as the results of ¹³C NMR analyses, the L₂PF resin had a more sufficient condensation between phenol, lignin, and formaldehyde, which led to a larger molecular structure and viscosity. The viscosity of L₁PF meets the Chinese National Standard (GB/T 14074-2017) and can be conveniently and effortlessly utilized in the wood manufacture.

The two plywood samples were prepared under 145 °C hot pressing and their performance is presented in Table 2. Generally, the bonding strength and formaldehyde emission of all the samples all reached the Chinese National Standard (GB/T 14074-2017). The heterogeneous macromolecular structure of lignin results in fewer active sites. The chemical structures of the cured resin adhesives are normally slightly unstable when replacing part of their content with lignin, and the bonding strength would be decreased as well. Especially, there were 24.6% other components in L₁ fraction, which could also hinder the condensation reaction. The bonding strength of the plywood bonded by L₁PF resin adhesive was lower than that by L₂PF resin adhesive, which correlated with the molecular structure differences of lignin and LPF resin adhesives. The bonding strength of all the samples tested reached the requirements of the exterior-grade panels (≥0.7 MPa). The wood failure of plywood bonded with LPF resin adhesives was shown in Fig. S8.

The formaldehyde emission of all the plywood by LPF resin adhesives was similar and markedly below 0.1 mg L⁻¹. This satisfactory formaldehyde emission not only lower than Chinese standard, but also lower than the highest standard of ISO and Japan. This was due to the fact that there existed only minimal amounts of unreacted formaldehyde in these LPF resin adhesives, which could be proven by the ¹³C NMR analyses in the previous section. Based on above results, the resin adhesive prepared using liquid lignin fraction shows desired performances and is satisfactory enough properties to sell in the current adhesive market. In summary, this production process provides a sustainable approach for the direct application of the liquid lignin fraction with minimal processing
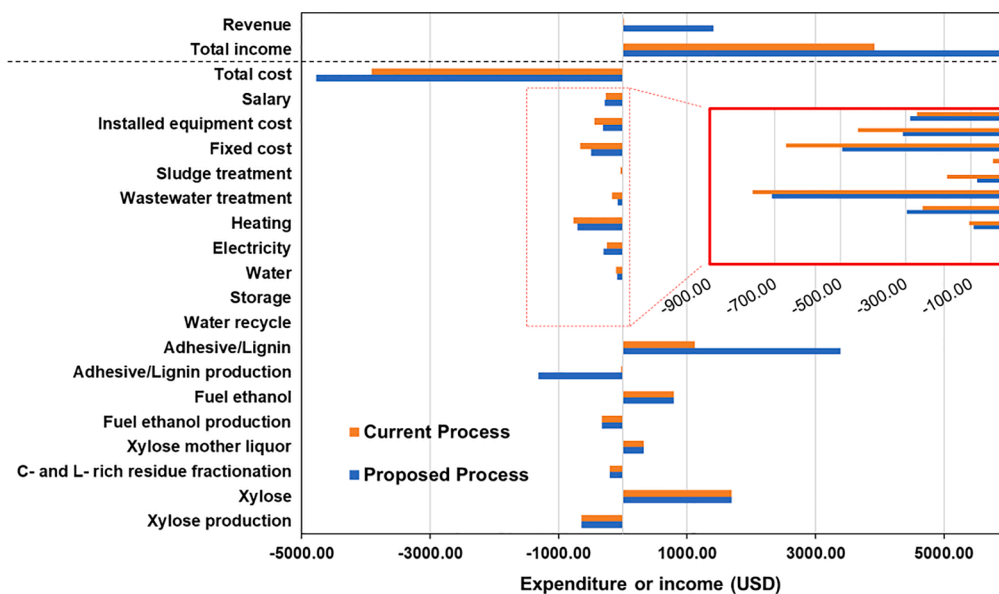
Fig. 5. Techno-economic analyses of the current process and the proposed EXA process.
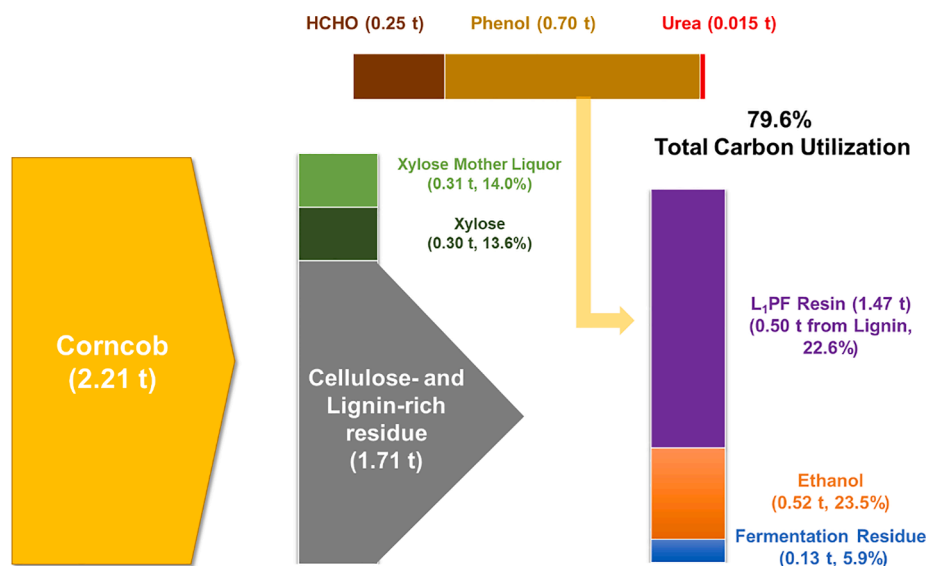

Fig. 6. Carbon flow chart of the proposed process (numbers in brackets mean carbon content in each fraction and the percentage based on the feedstock corncob). The mass (carbon) balance analysis was performed based on a plant-size process model of producing 1 t ethanol.

requirements.

3.2. Techno-economic and mass (carbon) balance analyses

To better assess the viability of the proposed strategy and techno-economic analyses were performed based on a plant-size process model of producing 1 t ethanol (Fig. 5). Detail information about economic parameters, energy input, capital, and operating costs could be found in the supplementary Tables (Tables S8–S11).

The costs of all stage mainly included the chemicals for each operating unit (Figs S1 and S2), the energy consumption, and the capital cost. The revenue of the current process is 12.71 USD (based on a plant-size process model of producing 1 t ethanol), which means the company has to rely on subsidies (for valorization of agricultural wastes) from local government to keep this project running (such as 84.58 USD/t ethanol in 2016). In contrast, the value-added products obtained from the proposed EXA process can result in a total income of 6186.23 USD

with an associated capital and operating cost of 4771.69 USD (Fig. 5 and Table S10). The overall revenue of EXA process reaches 1414.55 USD, which is 110 times projected increase compared with the current process. Among all the processing steps, the adhesive production step costs the most owing to the utilization of expensive phenol, which is compensated by the market value of the produced adhesive (Fig. S9). Therefore, the cost can be significantly reduced by developing alternative methods with higher substitution rate of lignin to phenol (only 50% in the current work). Moreover, regarding the recent work by Sels and co-workers [26], phenol can be also sustainably coproduced from lignin fraction of lignocellulosic biomass. Therefore, cheaper renewable phenol can likely be obtained in the near future. In addition, the hemicellulose can be used for the production of more valuable xylooligosaccharide (8457.66–38059.47 USD/t) and improving the total revenue further. In summary, the proposed EXA process can create appreciable revenues with limited investments due to its resemblance with the parent process and is facile and convenient to establish and
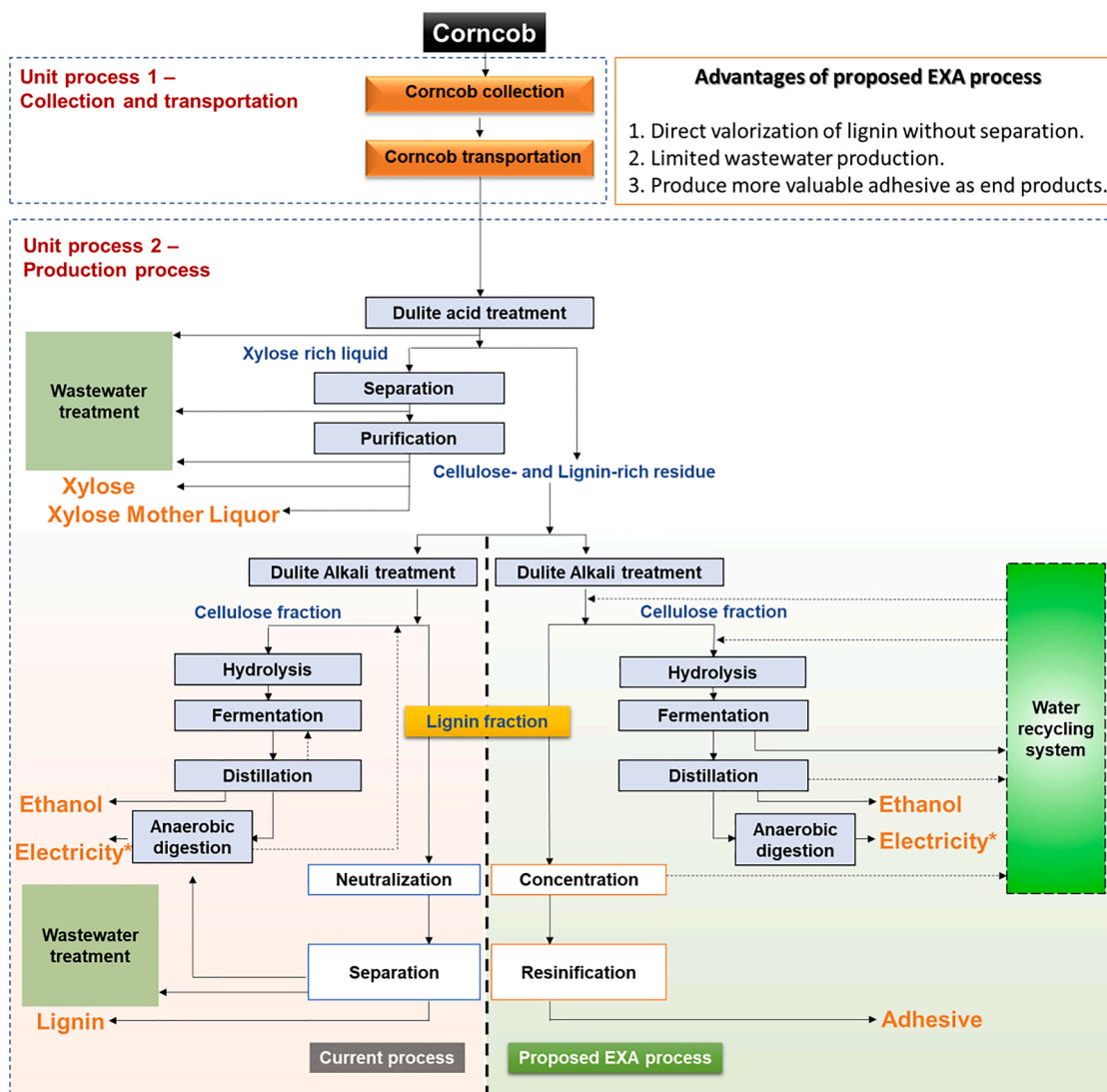
Fig. 7. "Cradle-to-gate" LCA system boundary for the current and proposed corncob biorefinery designs (dashed square indicates water recycling, energy and heat flows are not shown, *marks electricity produced from anaerobic digestion that is reused in the system).

operate even without government subsidy.

Calculated based on the elementary analysis results (Table S12), corncob with total carbon content of 2.21 t can be used to produce xylose (0.30 t C) and leaving cellulose- and lignin-rich residue (1.71 t C) that can be used for the production of ethanol (0.52 t C), and L_1PF resin adhesive (1.47 t C), respectively (Fig. 6). Xylose mother liquor (0.31 t C) containing the mixture of several hemicellulose derived sugars is another high-value customer product. Fermentation residue (0.13 t C) can be used as the filler for plywood. On the basis of the proposed EXA biorefinery, 79.6% of the renewable carbon in corncob can be economically and sustainably valorized into several high-value market imperative end-products. These yields are higher than those obtained by other strategies, such as the recent reported integrated biorefinery process for the production of phenol, propylene, oligomers, and pulp from wood (76%) [26].

Moreover, the proposed EXA process reduced waste water generation by 57.8% after cooperating a water recycling unit, which is also benefit for the environmental management. The proposed EXA process reduced the waste water from the lignin separation step. This improvement could significantly decrease the usage of chemicals for disposing the waste water, such as alkali and ferric trichloride. In addition, the proposed EXA process produced waste water that is more benign and thus can benefit to the anaerobic digestion. The equipment

of water recycling process mainly included the storage cylinder, delivery line, pump, and heat exchanger. The concentration process adopted multiple-effect evaporation. The evaporated water condensed through heat exchanger. The condensate water in storage cylinder could be transported to another process. The implementation of new processes is associated with technical risks, requires extra capital investments. The predicted net present value was calculated based on the production of 30000 t ethanol per year. The discount rate was set as 8.00%. The results show that there is a small fluctuation in the internal rate of return. However, the net present value of the proposed EXA process is apparently higher than the current process.

3.3. Life cycle assessment (LCA)

The two biorefinery processes share the same design for the dilute acid treatment and xylose production processes. The difference lays in the treatment of the cellulose- and lignin-rich residue. The current process yields lignin as a product after neutralization and separation while the EXA process produces L_1PF resin adhesive directly from lignin rich aqueous solution. Water recycling in the current design is limited whilst the system is optimized to recycle water in the EXA process which avoids production of large quantity of waste water after separation of lignin. According to the process flow diagram (Fig. 7), cellulose- and

Table 3

"Cradle-to-gate" GHG emission intensities for all products in the two corncob biorefinery design processes.[a]

GHG intensities	Unit	Current process	EXA process
Plant	t CO_2 eq.	16.1	19.9
Plant	t CO_2 eq./USD revenue	1.27	0.014
Ethanol	g CO_2 eq./MJ	132.8	111.7
Lignin	kg CO_2 eq./kg	2.90	–
L_1PF Adhesive	kg CO_2 eq./kg	–	1.82
Xylose	kg CO_2 eq./kg	6.91	6.71
Xylose mother liquor	kg CO_2 eq./kg	0.52	0.50

[a] In order to compare the two designs, GHG emissions emitted to process 5.25 t of dry corncobs were calculated and their intestines are also expressed as the amount per USD revenue generated.

lignin-rich residue and xylose-rich liquid are outputs of the acid treatment. Emissions associated with this process were allocated between them. The emissions associated with xylose production were allocated between xylose and liquor. For the current process, anaerobic digestion treats wastewater from both lignin and ethanol productions. Hence, alkaline treatment, lignin production, and ethanol production were treated as one subsystem. Emissions associated with it were allocated between final products, lignin and ethanol. As a result, environmental burdens from the dilute acid pretreatment were allocated to xylose processing residue (53.6%) and xylose-rich liquid (46.4%). Those from the dilute alkali treatment were allocated to ethanol (27.6%) and lignin (72.4%). For the proposed process, adhesive and ethanol productions were two separate subsystems post alkaline treatment. Therefore, emissions associated with alkaline treatment were allocated between cellulose pulp and lignin rich liquid. The economic values for all these intermediate products were estimated by the subsequent final products' prices and processes' costs. Emissions associated with anaerobic digestion in the current design were allocated between lignin and ethanol whilst emissions associated with water recycle in the proposed design were allocated between the L_1PF resin adhesives and ethanol based on their prices. The allocation percentages are 61.0% for the cellulose- and lignin-rich residue and 39.0% for xylose-rich liquid post dilute acid pretreatment whilst 14.7% for ethanol and 85.3% for the LPF resin adhesives post dilute alkali treatment.

Table 3 shows the calculated "cradle-to-gate" GHG intensities for all products in the two process designs. These "cradle-to-gate" results do not include GHG emissions from the end-use phase and biogenic carbon embedded in final products. Note that the GHG emission intensities of all products from both designs are not directly comparable due to differences in the economic allocation percentages. The results show that the total GHG emissions from the EXA process are higher than those of the current process, mainly due to the use of phenol, formaldehyde, and other chemicals in L_1PF resin adhesive production process. Nevertheless, GHG emission intensities expressed as kg CO_2 eq./USD revenue of the EXA process are significantly lower than the current process, showing an improvement from the environment-revenue effectiveness perspective.

To compare with conventional products (i.e. ethanol v.s. gasoline and lignin-based v.s. phenolic resin), the system boundary was expanded to include the end-use phase. Ethanol and gasoline were combusted in vehicle engines by assuming that all carbon in the fuels is converted to CO_2. Including 0.97 kg CO_2 eq./MJ distribution GHG intensity [40], the "cradle-to-grave" GHG intensities for ethanol are 132.8 g CO_2 eq./MJ in the current design and 111.7 g CO_2 eq./MJ in the proposed EXA process, compared to gasoline 90.2 g CO_2 eq./MJ [69]. The higher carbon intensities are mainly driven by coal-based steam (0.366 kg CO_2 eq./kg steam as the national average in China). Normally, second-generation ethanol has lower GHG intensity than gasoline due to the self-efficient operation and even surplus electricity credits as a result of the incineration of the lignin residue. In the EXA process, lignin was converted to produce value-added products (i.e. LPF resin adhesives
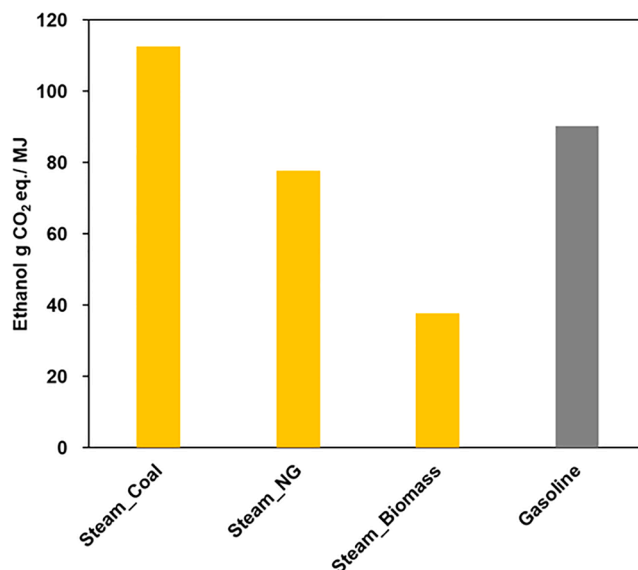

Fig. 8. Scenario analyses of the proposed biorefinery using alternative sources for steam generation (i.e. coal, natural gas, and biomass).

instead of energy. A perspective case study was performed to explore alternative low carbon fuel as the source for steam (i.e. natural gas and biomass Fig. 8). Results show that ethanol GHG intensity could be reduced significantly to 77.8 g CO_2 eq./MJ and 37.8 g CO_2 eq./MJ respectively, when using steam generated from natural gas and biomass (*e.g.* corncob onsite). The latter ethanol GHG intensity is close to its lower boundary (39.0–50.0 g CO_2 eq./MJ), the range from a conceptual design of corncob-based ethanol plant using lignin residue as the main energy source comparable to other second-generation biofuels [38].

The "cradle-to-gate" GHG intensity of L_1PF resin adhesive is 1.82 kg CO_2 eq./kg, compared to that of phenolic resin 4.58 kg CO_2 eq./kg. According to the Ecoinvnet database [70], conventional phenolic resin contains approx. 86% phenol and 14% formaldehyde. It is assumed that all non-biogenic carbon in L_1PF resin adhesive and those in the conventional phenolic resin were converted to CO_2 in the end use phase. The "cradle-to-grave" GHG intensity for L_1PF resin adhesive is 2.73 kg CO_2 eq./kg, compared to that of phenolic resin 7.99 kg CO_2 eq./kg, representing 66% GHG emissions saving. Credits from L_1PF resin adhesive replacing fossil-based resins should be considered when comparing the biorefinery design and the reference system (gasoline and fossil-based resin i.e. phenolic formaldehyde resin). Total "cradle-to-grave" GHG emissions from the proposed EXA process (25.4 t CO_2 eq.) are smaller than the reference system (50.3 t CO_2 eq.) though the ethanol GHG intensity is higher than gasoline on an energy basis. These results illustrate that the EXA biorefinery design delivers lower carbon footprint from a systematic perspective.

Contributions by input were analyzed for the proposed EXA process as an example and results are shown in Fig. 9. The results illustrate that steam generation is the biggest contributor, followed by electricity use for the dilute alkali treatment and the ethanol production steps; or chemicals use for the production of lignin-based adhesives and xylose. It is suggested that the use of alternative low carbon-based steam (Fig. 8) and chemicals or the recycling of chemicals (*excl.* adhesive production where chemicals are components in output) could reduce total GHG emissions of the proposed design and further improve its environmental performance.

A sensitivity analysis was also performed to quantify the effect of fluctuations in parameters i.e. co-products' prices (varied by 10%) on the carbon intensity of ethanol, following the one-at-a-time (OAT) approach (Fig. 10). The sensitivity ratio (SR) was calculated for each parameter following the equation below [26].
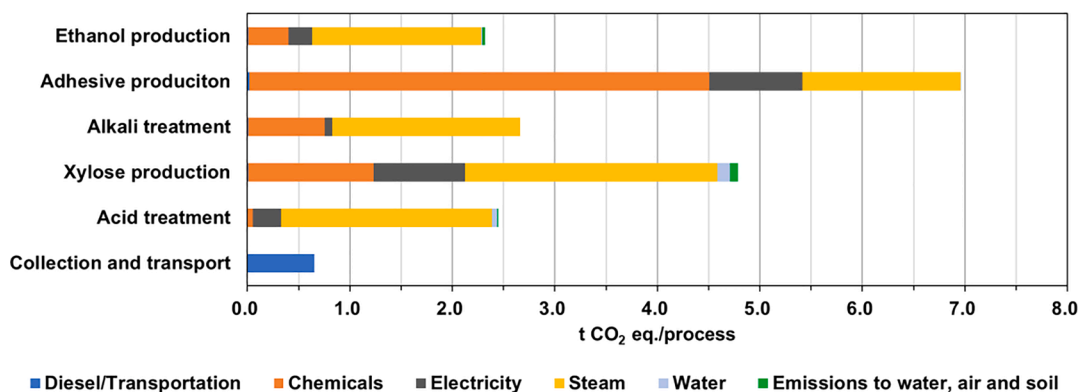
Fig. 9. Contribution analysis of the proposed EXA process design (t CO$_2$ eq. / 5.25 t processed corncob).
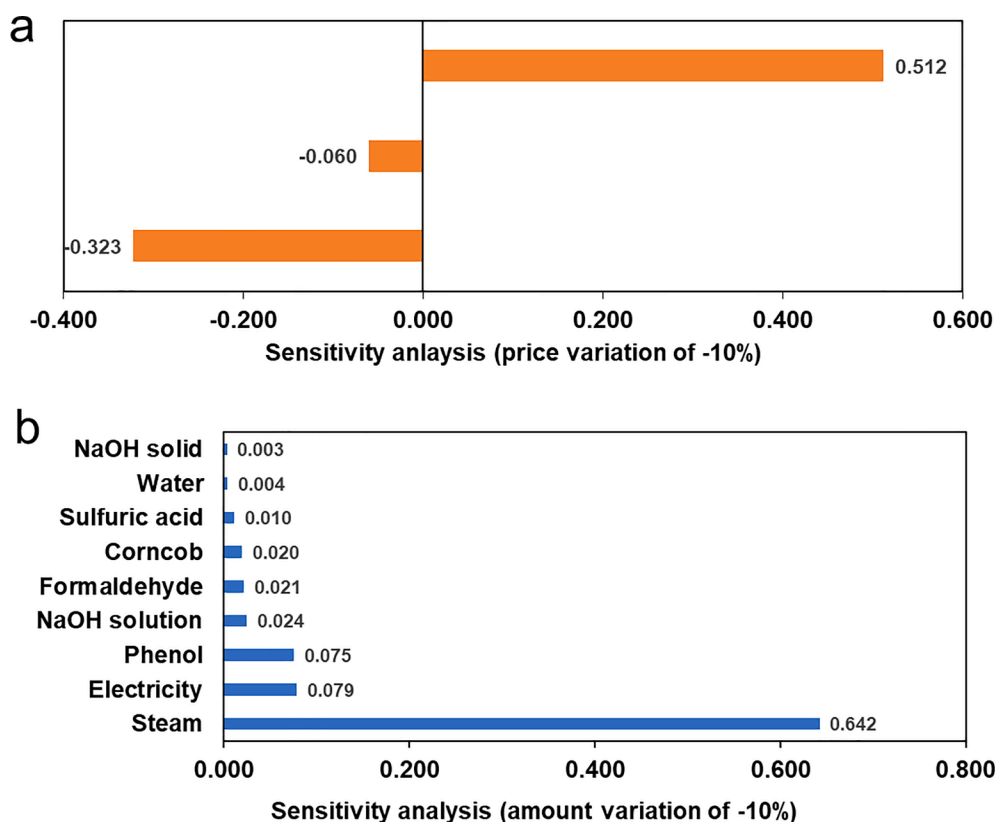

Fig. 10. The impact of the changes of parameters on the GHG intensity of ethanol. a. Sensitivity ratio with −10% price variation, b. Sensitivity ratio with −10% amount variation.

Sensitivity ratio = ($\triangle$results/Initial results)/($\triangle$parameter/Initial parameter)

The impact of products' prices on the GHG intensity of ethanol is due to the resulted changes in economic allocation ratios. With the decrease in ethanol price, fewer environmental burdens from acid and alkali treatment were allocated to the ethanol production process. On the contrary, the decreased price of L$_1$PF resin adhesive or xylose will result in more burdens being assigned to ethanol. The reduced amount of inputs will alter both total GHG emissions from the system and change the economic allocation percentages. The results reflect the combination of these impacts, showing that the most sensitive factor is the steam consumption followed by electricity use.

In summary, a life cycle assessment for two corncob biorefinery process designs were performed in addition to the techno-economic analysis. The proposed process uses approximately 15% less water

than the current process because of benefits from the water recycling system. Though the total GHG emissions from the proposed design are higher than those from the current process, its GHG emissions intensity per USD generated is lower, demonstrating the proposed system is more efficient from an environment-revenue perspective. The "cradle-to-gate" GHG intensities (excl. the end use phase and biogenic carbon) for all products from the proposed design are 111.7 g CO$_2$ eq./MJ ethanol, 6.71 kg CO$_2$ eq./kg xylose, 1.82 kg CO$_2$ eq./kg adhesive and 0.50 kg CO$_2$ eq./kg xylose mother liquor. The "cradle-to-grave" GHG intensity for L$_1$PF resin adhesive is about 2.73 kg CO$_2$ eq./kg, compared to that of phenolic resin 7.99 kg CO$_2$ eq./kg, representing 66% GHG emissions saving. By altering steam source from coal to biomass, the "cradle-to-grave" GHG intensity of ethanol could achieve 37.78 g CO$_2$ eq./MJ, delivering approx. 60% GHG reduction against gasoline (90.20 g CO$_2$ eq./MJ of gasoline as shown in S10).

4. Conclusions

In this study, the EXA process transforming waste corncob to xylose, ethanol, and valuable adhesive is proposed. Compared with other processes either using lignin or cellulose first, this process first transforms hemicellulose to xylose while keeping good quality of cellulose and lignin for further valorization. All lignocellulose components are valorized with an overall total carbon utilization of 79.6% for the named products, which shows a promising atom-economic process design. This EXA biorefinery process includes four stages. Stage 1 focuses on direct production of xylose from hemicellulose. Stage 2 deals with processing of the cellulose- and lignin-rich residue by dilute alkali fractionation. This stage yields high quality cellulose that can be converted to ethanol (stage 3) as well as a high-lignin containing liquor that is converted to a lignin-based phenol formaldehyde (LPF) resin adhesive in stage 4. In contrast to other lignin-rich liquors that often contain hemicellulose derived components and thus require another lignin purification step before application, the lignin liquor obtained from the EXA process can be directly used after a simple concentration step. This means significant energy savings and an overall simplification of the processing steps. It is worth mentioning that other similar lignin based adhesive production factories can potentially utilize our strategy to directly use high-lignin containing liquor as raw material. However, the pH and lignin activity of the liquor should be considered and we worked for a long time to figure out the optimum operation procedures for the EXA process. Similar balancing is likely required for other processes. The produced adhesive has satisfactory performances of all properties meet the Chinese National Standard and can be used in wood manufacture with good selling price in the market. The direct utilization of concentrated lignin fractionation also reduces waste-water generation and the subsequent treatment significantly. Thus, the presented EXA process is more environmental-friendly.

Techno-economic analysis and life cycle assessment were then applied for analyzing both the current and proposed EXA processes. The overall revenue of the EXA biorefinery process reached 1414.55 USD, increased significantly as compared with the current process (12.71 USD). GHG intensities obtained from life cycle assessment shows a much lower GHG emissions intensity per USD than the current process (0.014 vs 1.27 t CO_2 eq./USD revenue), demonstrating a more cost-effective process design from an environment-revenue perspective.

Although the proposed EXA process starts from agricultural waste corncob, it can be easily shifted to other feedstocks like wheat straw and corn stalks as these all contain a similar composition of major components. There is no doubt that this process will achieve great success and generating more profitable, sustainable, low-carbon footprint chemicals, and materials in the near future.

Declaration of Competing Interest

The authors declare that they have no known competing financial interests or personal relationships that could have appeared to influence the work reported in this paper.

Acknowledgements

Appendix A. Supplementary data

Supplementary data to this article can be found online at https://doi.org/10.1016/j.cej.2021.129565.

References

[1] J. Channell, E. Curmi, Z. Whitton, E. McKinnon, T.M. Fordham, United Nations Sustainable Development Goals, 2018. www.citi.com/citigps.
[2] J.E. Trancik, Back the renewables boom, Nature 507 (2014) 300–302, https://doi.org/10.1038/507300a.
[3] C.O. Tuck, E. Perez, I.T. Horvath, R.A. Sheldon, M. Poliakoff, Valorization of biomass: deriving more value from waste, Science 337 (6095) (2012) 695–699, https://doi.org/10.1126/science:1218930.
[4] K. Sanderson, Lignocellulose: a chewy problem, Nature. 474 (7352) (2011) S12–S14, https://doi.org/10.1038/474S012a.
[5] J.S. Luterbacher, D. Martin Alonso, J.A. Dumesic, Targeted chemical upgrading of lignocellulosic biomass to platform molecules, Green Chem. 16 (12) (2014) 4816–4838, https://doi.org/10.1039/C4GC01160K.
[6] A.J. Ragauskas, C.K. Williams, B.H. Davison, G. Britovsek, J. Cairney, C.A. Eckert, W.J.F. Jr, J.P. Hallett, D.J. Leak, C.L. Liotta, J.R. Mielenz, R. Murphy, R. Templer, T. Tschaplinski, The path forward for biofuels and biomaterials, Science 311 (2006) 484–489, https://doi.org/10.1126/science.1114736.
[7] L. Petridis, J.C. Smith, Molecular-level driving forces in lignocellulosic biomass deconstruction for bioenergy, Nat. Rev. Chem. 2 (11) (2018) 382–389, https://doi.org/10.1038/s41570-018-0050-6.
[8] Y.M. Questell-Santiago, M.V. Galkin, K. Barta, J.S. Luterbacher, Stabilization strategies in biomass depolymerization using chemical functionalization, Nat. Rev. Chem. 4 (6) (2020) 311–330, https://doi.org/10.1038/s41570-020-0187-y.
[9] L. Wang, M. Sharifzadeh, R. Templer, R.J. Murphy, Technology performance and economic feasibility of bioethanol production from various waste papers, Energy Environ. Sci. 5 (2) (2012) 5717–5730, https://doi.org/10.1039/C2EE02935A.
[10] L. Wang, R. Templer, R.J. Murphy, Environmental sustainability of bioethanol production from waste papers: Sensitivity to the system boundary, Energy Environ. Sci. 5 (2012) 8281–8293, https://doi.org/10.1039/c2ee21550k.
[11] A.J. Ragauskas, G.T. Beckham, M.J. Biddy, R. Chandra, F. Chen, M.F. Davis, B.H. Davison, R.A. Dixon, P. Gilna, M. Keller, P. Langan, A.K. Naskar, J.N. Saddler, T.J. Tschaplinski, G.A. Tuskan, C.E. Wyman, Lignin valorization: improving lignin processing in the biorefinery, Science. 344 (2014) 1246843. https://doi.org/10.1126/science.1246843.
[12] S.O. Limarta, H. Kim, J.-M. Ha, Y.-K. Park, J. Jae, High-quality and phenolic monomer-rich bio-oil production from lignin in supercritical ethanol over synergistic Ru and Mg-Zr-oxide catalysts, Chem. Eng. J. 396 (2020) 125175, https://doi.org/10.1016/j.cej.2020.125175.
[13] T. Ren, S. You, M. Zhang, Y. Wang, W. Qi, R. Su, Z. He, Improved conversion efficiency of lignin-to-fuel conversion by limiting catalyst deactivation, Chem. Eng. J. 410 (2021) 128270, https://doi.org/10.1016/j.cej.2020.128270.
[14] Z. Sun, K. Barta, Cleave and couple: toward fully sustainable catalytic conversion of lignocellulose to value added building blocks and fuels, Chem. Commun. 54 (56) (2018) 7725–7745, https://doi.org/10.1039/C8CC02937G.
[15] R. Rinaldi, R. Jastrzebski, M.T. Clough, J. Ralph, M. Kennema, P.C.A. Bruijnincx, B.M. Weckhuysen, Paving the way for lignin valorisation: recent advances in bioengineering, biorefining and catalysis, Angew. Chemie – Int. Ed. 55 (29) (2016) 8164–8215, https://doi.org/10.1002/anie.201510351.
[16] Z. Sun, B. Fridrich, A. de Santi, S. Elangovan, K. Barta, Bright side of lignin depolymerization: toward new platform chemicals, Chem. Rev. 118 (2) (2018) 614–678, https://doi.org/10.1021/acs.chemrev.7b00588.
[17] W. Schutyser, T. Renders, S. Van den Bosch, S.-F. Koelewijn, G.T. Beckham, B.F. Sels, Chemicals from lignin: an interplay of lignocellulose fractionation, depolymerisation, and upgrading, Chem. Soc. Rev. 47 (3) (2018) 852–908, https://doi.org/10.1039/C7CS00566K.
[18] Li. Shuai, M.T. Amiri, Y.M. Questell-Santiago, F. Héroguel, Y. Li, H. Kim, R. Meilan, C. Chapple, J. Ralph, J.S. Luterbacher, Formaldehyde stabilization facilitates lignin monomer production during biomass depolymerization, Sceince 354 (6310) (2016) 329–333, https://doi.org/10.1126/science.aaf7810.
[19] Y. Liu, L. Chen, T. Wang, Q.i. Zhang, C. Wang, J. Yan, L. Ma, One-pot catalytic conversion of raw lignocellulosic biomass into gasoline alkanes and chemicals over LiTaMoO6 and Ru/C in aqueous phosphoric acid, ACS Sustain. Chem. Eng. 3 (8) (2015) 1745–1755, https://doi.org/10.1021/acssuschemeng.5b00256.
[20] T.D. Matson, K. Barta, A.V. Iretskii, P.C. Ford, One-pot catalytic conversion of cellulose and of woody biomass solids to liquid fuels, J. Am. Chem. Soc. 133 (35) (2011) 14090–14097.
[21] Q. Xia, Z. Chen, Y. Shao, X. Gong, H. Wang, X. Liu, S.F. Parker, X. Han, S. Yang, Y. Wang, Direct hydrodeoxygenation of raw woody biomass into liquid alkanes, Nat. Commun. 7 (2016) 11602, https://doi.org/10.1038/ncomms11162.
[22] S. Van den Bosch, W. Schutyser, R. Vanholme, T. Driessen, S.-F. Koelewijn, T. Renders, B. De Meester, W.J.J. Huijgen, W. Dehaen, C.M. Courtin, B. Lagrain, W. Boerjan, B.F. Sels, Reductive lignocellulose fractionation into soluble lignin-derived phenolic monomers and dimers and processable carbohydrate pulps, Energy Environ. Sci. 8 (6) (2015) 1748–1763, https://doi.org/10.1039/C5EE00204D.
[23] M.M. Abu-Omar, K. Barta, G.T. Beckham, J.S. Luterbacher, J. Ralph, R. Rinaldi, Y. Román-Leshkov, J.S.M. Samec, B.F. Sels, F. Wang, Guidelines for performing lignin-first biorefining, Energy Environ. Sci. 14 (1) (2021) 262–292, https://doi.org/10.1039/D0EE02870C.
[24] Z. Sun, G. Bottari, A. Afanasenko, M.C.A. Stuart, P.J. Deuss, B. Fridrich, K. Barta, Complete lignocellulose conversion with integrated catalyst recycling yielding valuable aromatics and fuels, Nat. Catal. 1 (1) (2018) 82–92, https://doi.org/10.1038/s41929-017-0007-z.
[25] X. Wu, X. Fan, S. Xie, J. Lin, J. Cheng, Q. Zhang, L. Chen, Y.e. Wang, Solar energy-driven lignin-first approach to full utilization of lignocellulosic biomass under mild

conditions, Nat. Catal. 1 (10) (2018) 772–780, https://doi.org/10.1038/s41929-018-0148-8.

[26] Y. Liao, S.-F. Koelewijn, G. Van den Bossche, J. Van Aelst, S. Van den Bosch, T. Renders, K. Navare, T. Nicolaï, K. Van Aelst, M. Maesen, H. Matsushima, J. M. Thevelein, K. Van Acker, B. Lagrain, D. Verboekend, B.F. Sels, A sustainable wood biorefinery for low–carbon footprint chemicals production, Science 367 (6484) (2020) 1385–1390, https://doi.org/10.1126/science:aau1567.

[27] T. Renders, G. Van den Bossche, T. Vangeel, K. Van Aelst, B. Sels, Reductive catalytic fractionation: state of the art of the lignin-first biorefinery, Curr. Opin. Biotechnol. 56 (2019) 193–201, https://doi.org/10.1016/j.copbio.2018.12.005.

[28] Z. Sun, J. Cheng, D. Wang, T.-Q. Yuan, G. Song, K. Barta, Downstream processing strategies for the lignin-first biorefinery, ChemSusChem 13 (2020) 5199–5212, https://doi.org/10.1002/cssc.202002040.

[29] T. Renders, S. Van den Bosch, S.-F. Koelewijn, W. Schutyser, B.F. Sels, Lignin-first biomass fractionation: the advent of active stabilisation strategies, Energy Environ. Sci. 10 (7) (2017) 1551–1557, https://doi.org/10.1039/C7EE01298E.

[30] S.S. Gori, M.V.R. Raju, D.A. Fonseca, J. Satyavolu, C.T. Burns, M.H. Nantz, Isolation of C5-sugars from the hemicellulose-rich hydrolyzate of distillers dried grains, ACS Sustain. Chem. Eng. 3 (10) (2015) 2452–2457, https://doi.org/10.1021/acssuschemeng.5b00490.

[31] X. Ji, H. Ma, Z. Tian, G. Lyu, G. Fang, J. Chen, H.A.M. Saeed, Production of xylose from diluted sulfuric acid hydrolysis of wheat straw, BioResources 12 (2017) 7084–7095. https://doi.org/10.15376/biores.12.4.7084-7095.

[32] Y. Luo, Z. Li, X. Li, X. Liu, J. Fan, J.H. Clark, C. Hu, The production of furfural directly from hemicellulose in lignocellulosic biomass: a review, Catal. Today 319 (2019) 14–24, https://doi.org/10.1016/j.cattod.2018.06.042.

[33] Y. Yu, Y. Wan, H. Shang, B. Wang, P. Zhang, Y. Feng, Corncob-to-xylose residue (CCXR) derived porous biochar as an excellent adsorbent to remove organic dyes from wastewater, Surf. Interface Anal. 51 (2) (2019) 234–245, https://doi.org/10.1002/sia.6575.

[34] A. Sluiter, B. Hames, R. Ruiz, C. Scarlata, J. Slui, D. Templeton, D. Crocker, Determination of structural carbohydrates and lignin in biomass, 2008. http://www.nrel.gov/biomass/pdfs/42618.pdf.

[35] J.-L. Wen, S.-L. Sun, B.-L. Xue, R.-C. Sun, Quantitative structures and thermal properties of birch lignins after ionic liquid pretreatment, J. Agric. Food Chem. 61 (3) (2013) 635–645, https://doi.org/10.1021/jf3051939.

[36] J.-L. Wen, S.-L. Sun, T.-Q. Yuan, R.-C. Sun, Structural elucidation of whole lignin from Eucalyptus based on preswelling and enzymatic hydrolysis, Green Chem. 17 (3) (2015) 1589–1596, https://doi.org/10.1039/C4GC01889C.

[37] I.O. for Standardization, Environmental management: life cycle assessment; principles and framework, ISO, 2006.

[38] Y.U. Wang, M.-H. Cheng, M.M. Wright, Lifecycle energy consumption and greenhouse gas emissions from corncob ethanol in China, Biofuels, Bioprod. Biorefining. 12 (6) (2018) 1037–1046, https://doi.org/10.1002/bbb.2019.12.issue-610.1002/bbb.1920.

[39] WebLCA, (n.d.). https://www.weblca.net/home.

[40] GREET 2018 model, (n.d.). https://greet.es.anl.gov/.

[41] IPCC AR4 Report, (2007). https://www.ipcc.ch/assessment-report/ar4/.

[42] P. Xu M. Luo Xylose: production, consumption, and health benefits Nova Science Publishers 2012 https://books.google.es/books?id=KHDkygAACAAJ.

[43] Xylose – A Sweet Solution to Achieve Sugar Reduction, 2019. https://www.transparencymarketresearch.com/xylose-market.html.

[44] H.-J. Zhang, X.-G. Fan, X.-L. Qiu, Q.-X. Zhang, W.-Y. Wang, S.-X. Li, L.-H. Deng, M. A.G. Koffas, D.-S. Wei, Q.-P. Yuan, A novel cleaning process for industrial production of xylose in pilot scale from corncob by using screw-steam-explosive extruder, Bioprocess Biosyst. Eng. 37 (12) (2014) 2425–2436, https://doi.org/10.1007/s00449-014-1219-0.

[45] H. Li, A. Deng, J. Ren, C. Liu, Q. Lu, L. Zhong, F. Peng, R. Sun, Catalytic hydrothermal pretreatment of corncob into xylose and furfural via solid acid catalyst, Bioresour. Technol. 158 (2014) 313–320, https://doi.org/10.1016/j.biortech.2014.02.059.

[46] Z.H. Liu, H.Z. Chen, Xylose production from corn stover biomass by steam explosion combined with enzymatic digestibility, Bioresour. Technol. 193 (2015) 345–356, https://doi.org/10.1016/j.biortech.2015.06.114.

[47] B.P. Lavarack, G.J. Griffin, D. Rodman, The acid hydrolysis of sugarcane bagasse hemicellulose to produce xylose, arabinose, glucose and other products, Biomass and Bioenergy 23 (5) (2002) 367–380, https://doi.org/10.1016/S0961-9534(02)00066-1.

[48] B. Liu, T. Li, W. Wang, L.M.C. Sagis, Q. Yuan, X. Lei, M.A. Cohen Stuart, D. Li, C. Bao, J. Bai, Z. Yu, F. Ren, Y. Li, Corncob cellulose nanosphere as an eco-friendly detergent, Nat. Sustain. 3 (6) (2020) 448–458, https://doi.org/10.1038/s41893-020-0501-1.

[49] Q. Meng, S. Wu, C. Shen, Polyethylenimine-grafted-corncob as a multifunctional biomaterial for removing heavy metal ions and killing bacteria from water, Ind. Eng. Chem. Res. 59 (39) (2020) 17476–17482, https://doi.org/10.1021/acs.iecr.9b06606.

[50] I. Egüés, A.M. Stepan, A. Eceiza, G. Toriz, P. Gatenholm, J. Labidi, Corncob arabinoxylan for new materials, Carbohydr. Polym. 102 (2014) 12–20, https://doi.org/10.1016/j.carbpol.2013.11.011.

[51] A. Gupta, J.P. Verma, Sustainable bio-ethanol production from agro-residues: A review, Renew. Sustain. Energy Rev. 41 (2015) 550–567, https://doi.org/10.1016/j.rser.2014.08.032.

[52] S. Gao, Z. Cheng, X.i. Zhou, Y. Liu, J. Wang, C. Wang, F. Chu, F. Xu, D. Zhang, Fabrication of lignin based renewable dynamic networks and its applications as self-healing, antifungal and conductive adhesives, Chem. Eng. J. 394 (2020) 124896, https://doi.org/10.1016/j.cej.2020.124896.

[53] W. Wang, F. Wang, C. Zhang, J. Tang, X. Zeng, X. Wan, Versatile value-added application of hyperbranched lignin derivatives: water-resistance adhesive, UV protection coating, self-healing and skin-adhesive sensing, Chem. Eng. J. 404 (2021) 126358, https://doi.org/10.1016/j.cej.2020.126358.

[54] A. Tejado, C. Peña, J. Labidi, J.M. Echeverria, I. Mondragon, Physico-chemical characterization of lignins from different sources for use in phenol – formaldehyde resin synthesis, Bioresour. Technol. 98 (8) (2007) 1655–1663, https://doi.org/10.1016/j.biortech.2006.05.042.

[55] IHS Markit Customer Care, Phenolic resins, 2018.

[56] Grand View Research, Global wood adhesives market size, share, industry report, 2025, 2019.

[57] S. Yang, Y. Zhang, T.Q. Yuan, R.C. Sun, Lignin-phenol-formaldehyde resin adhesives prepared with biorefinery technical lignins, J. Appl. Polym. Sci. 132 (2015) 42493(1–8). https://doi.org/10.1002/app.42493.

[58] B.O. Pang, S.S. Lam, X.-J. Shen, X.-F. Cao, S.-J. Liu, T.-Q. Yuan, R.-C. Sun, Valorization of technical lignin for the production of desirable resins with high substitution rate and controllable viscosity, ChemSusChem 13 (17) (2020) 4446–4454, https://doi.org/10.1002/cssc.v13.1710.1002/cssc.202000299.

[59] B.o. Pang, X.-F. Cao, S.-N. Sun, X.-L. Wang, J.-L. Wen, S.S. Lam, T.-Q. Yuan, R.-C. Sun, The direct transformation of bioethanol fermentation residues for production of high-quality resins, Green Chem. 22 (2) (2020) 439–447, https://doi.org/10.1039/C9GC03568K.

[60] D. Kai, M.J. Tan, P.L. Chee, Y.K. Chua, Y.L. Yap, X.J. Loh, Towards lignin-based functional materials in a sustainable world, Green Chem. 18 (5) (2016) 1175–1200, https://doi.org/10.1039/C5GC02616D.

[61] I. Poljanšek, U. Šebenik, M. Krajnc, Characterization of phenol–urea–formaldehyde resin by inline FTIR spectroscopy, J. Appl. Polym. Sci. 99 (5) (2006) 2016–2028, https://doi.org/10.1002/app.v99:510.1002/app.22161.

[62] B. Park, B. Riedl, 13C-NMR study on cure-accelerated phenol-formaldehyde resins with carbonates, J. Appl. Polym. Sci. 77 (2000) 1284–1293, https://doi.org/10.1002/(SICI)1097-4628(20000725).

[63] B. Tomita, S. Hatono, Urea-formaldehyde resins. III. Constitutional characterization by 13C fourier transform NMR spectroscopy, J. Polym. Sci. Part A 16 (1978) 2509–2525, https://doi.org/10.1002/pol.1978.170161040.

[64] C. Zhao, A. Pizzi, S. Garnier, Fast advancement and hardening acceleration of low-condensation alkaline PF resins by esters and copolymerized urea, J. Appl. Polym. Sci. 74 (1999) 359–378, https://doi.org/10.1002/(SICI)1097-4628(20000711).

[65] Y. Zhao, N. Yan, M.W. Feng, Thermal degradation characteristics of phenol-formaldehyde resins derived from beetle infested pine barks, Thermochim. Acta 555 (2013) 46–52, https://doi.org/10.1016/j.tca.2012.12.002.

[66] Mozaffar Alam Khan, Sayed Marghoob Ashraf, Ved Prakash Malhotra, Development and characterization of a wood adhesive using bagasse lignin, Int. J. Adhes. Adhes. 24 (6) (2004) 485–493, https://doi.org/10.1016/j.ijadhadh.2004.01.003.

[67] W. Lee, K. Chang, I. Tseng, Properties of phenol-formaldehyde resins prepared from phenol-liquefied lignin, J. Appl. Polym. Sci. 124 (2011) 4782–4788, https://doi.org/10.1002/app.35539.

[68] W. Zhang, Y. Ma, C. Wang, S. Li, M. Zhang, F. Chu, Preparation and properties of lignin – phenol – formaldehyde resins based on different biorefinery residues of agricultural biomass, Ind. Crop. Prod. 43 (2013) 326–333, https://doi.org/10.1016/j.indcrop.2012.07.037.

[69] T. Peng, S. Zhou, Z. Yuan, X. Ou, Life cycle greenhouse gas analysis of multiple vehicle fuel pathways in China, Sustainability 9 (2017) 2183, https://doi.org/10.3390/su9122183.

[70] Life cycle inventories of chemicals, (2007). https://db.ecoinvent.org/reports/08_Chemicals.pdf.